ACS APPLIED MATERIALS & INTERFACES

Research Article

www.acsami.org

Characteristics of Colored Passive Layers on Titanium: Morphology, Optical Properties, and Corrosion Resistance

Rebecca J. Holmberg, Diane Beauchemin,* and Gregory Jerkiewicz*

Department of Chemistry, Queen's University, 90 Bader Lane, Kingston, Ontario, Canada K7L 3N6

ABSTRACT: Electrochemically formed colored passive layers on titanium and their optical, surface morphology, and corrosion properties are presented and discussed. With the application of progressively higher AC voltages (V_{AC}) during preparation of these passive layers, they are found to become more protective of the underlying metal, as determined from corrosion resistance measurements employing electrochemical polarization curve and inductively coupled plasma mass spectrometry experiments. The passive layers on titanium were found to be uniform in their surface morphology with no apparent cracks or pits. Surface morphology, and its relation to optical properties, was also investigated using visible light microscopy, profilometry, and near-infrared ultraviolet visible reflectance spectroscopy measurements. A correlation between the light reflected from the entire sample surface and the coloration of surface grains was also observed through these measurements. The reflectance spectra showed a red-shift of wavelength maxima (λ_{max}) values as AC voltages and, therefore, thicknesses were increased. Overall, these passive layers are protective of an already remarkable metal, and with greater knowledge of the properties of colored protective layers, their potential may be employed in a wide range of applications.

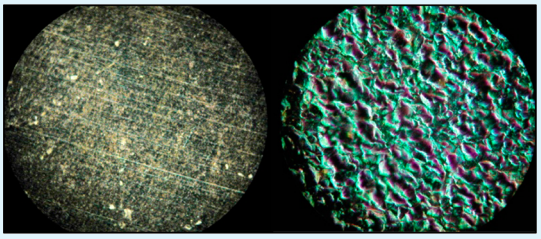

KEYWORDS: *titanium, colored passive layers, AC polarization, morphology, inductively coupled plasma mass spectrometry, corrosion, electrochemical characteristics*

INTRODUCTION

Titanium (Ti) due to its remarkably high strength, relatively high hardness (6.0 on the Mohs scale), corrosion resistance in seawater as well as in aqueous acidic and alkaline media, temperature resistance, low density, etc., finds a wide range of applications in industries that span from aerospace and marine, through medical, to nuclear waste storage.[1−5] Titanium is often analyzed for its mechanical and corrosion-related properties in various gaseous and liquid media in order to assess its suitability as a construction or other material and to find new applications. A method that arose to improve the corrosion resistance of Ti while offering decorative properties (surface coloration) was the formation of a protective passive layer through thermal or electrochemical means.[6,7] Since electrochemical passivation was far more energy efficient and produced more evenly coated and consistent layers, it became the preferred method.[8−14] The method employed by Jerkiewicz et al.[15] involved the use of AC voltage instead of the previously employed DC voltage and an aqueous solution of NH_4BF_4. It produced compact, more brightly and uniformly colored passive layers, and thus was preferable to the previous method.

Zhao et al.[16,17] performed experiments on Ti passivation using the AC voltage method in order to prepare biocompatible layers that would make it suitable for dental and orthodontic applications. It was found that the passive layers on Ti and Ti-based alloys significantly improved their corrosion and biocorrosion resistance as compared to the untreated metal.[18,19] This led to the body of work reported in this contribution, where the focus was on applications in aesthetics (contribution to the observed coloration), as well as applications in marine, aerospace, automotive, and medical industries (saline solution corrosion testing and its relation to the surface structure).

Elsewhere, it was shown that the passive layers' thickness and coloration can be fine-tuned by adjusting the applied AC voltage.[17,20] Their chemical composition and thickness can be evaluated using X-ray photoelectron spectroscopy (XPS) coupled with Ar-ion depth profiling. It was shown that the chemical composition of the colored passive layers on Ti gradually changes from TiO at the inner metal/passive layer to Ti_2O_3 in the intermediate layer, and TiO_2 in the outermost layer. A small amount of Ti fluoride was also found in the inner and intermediate layers; it originated from the decomposition of the NH_4BF_4 electrolyte solution.[14]

We previously published an extensive study on the electrochemical passivation of Zr and the resulting properties achieved.[21] Although Ti and Zr possess many similar properties, they still reveal certain differences, such as grain structure and size, that are of particular relevance to this research. In this contribution, we present a detailed electrochemical method for the formation of colored passive layers on Ti and examine how their visual properties (coloration) depend on the sample pretreatment (polishing versus etching). We report new data on the optical properties, surface morphology,

Received: September 24, 2014
Accepted: November 17, 2014
Published: November 17, 2014

and corrosion resistance in relation to the applied preparation and experimental conditions. We examine the stability of the passive layers under corrosion-promoting conditions using inductively coupled plasma mass spectrometry and electrochemical techniques. Finally, we compare the results achieved using Ti with those obtained using Zr.

EXPERIMENTAL SECTION

Titanium Electrodes, Electrolyte, and Cell. The following research was carried out using circular, square, and wire-shaped titanium samples, and all preparation methods were similar to those published in our previous work on Zr.[21] In particular, circular and square electrodes were most commonly employed in characterization of the coloration and morphology of Ti samples, whereas electrochemical studies were performed using wire-shaped electrodes. Ti electrodes were cut to be either 7 or 10 mm in diameter and 0.890 mm (0.035 in.) in thickness from a Ti sheet (Johnson-Matthey, 99.7 wt % containing 0.0875% Fe, 0.1225% O, 0.0015% N, 0.0095% C, and 0.0023% H). In order to be passivated, the electrodes were then spot-welded to a Ti wire (Aldrich, 99.7 wt %) for electrical contact. All employed electrodes were degreased in acetone under reflux in order to remove any organic impurities that originate from handling and shipping. Subsequently, electrodes were etched for an average of 7−12 min in a solution of 30 cm^3 of concentrated HF and 50 cm^3 of concentrated HNO_3 diluted to 1000 cm^3 with ultra-high-purity (UHP) water (Millipore 18.2 MΩ cm). Electrodes were thoroughly washed of the etchant solution with UHP water following this process. Wire-shaped electrodes were cut from Ti wire (Aldrich, 99.7% wt and 0.81 ± 0.02 mm in diameter). As these wire electrodes were employed for electrochemical measurements, they were connected to copper wire through an electric connector. The Ti wire−copper wire connection was sealed with epoxy resin (Struers), and only the Ti wire portion was in contact with electrolyte. Once the epoxy resin was hardened, Ti wire was cut to a length of 1.00 ± 0.05 cm and subsequently polished at the incision using sandpaper on a mechanical polisher (Struers) in order to reach a flat end. Removal of any residue from the preparation process was achieved through acetone degreasing and rinsing with UHP water. Wire electrodes were then treated in the etching solution described above, rinsed with UHP water, and sonicated in an ultrasonic bath (Branson) for 1 min. All Ti electrodes were immersed in a single compartment electrochemical cell where the electrochemical coloration was carried out by application of AC voltage (V_{AC}).[15,21] A counter electrode of Pt foil spot-welded to a Pt wire (Johnson-Matthey, 99.9 wt %) was employed; with a real surface area of a minimum 10 times greater than that of the Ti electrode. The distance between the working (Ti) and counter (Pt) electrodes was maintained at ca. 5 cm, this separation being sufficient in order to promote effective electrolyte circulation between electrodes, and for removal of any gases potentially generated during AC polarization. The procedure for preparing Ti samples throughout the course of research ensured reproducibility of experimental results and was consistent with the methodology used to prepare Zr samples.[21] During AC polarization, the cell was placed in a water bath, with a stream of N_2(g) being passed through it, in order to achieve successful control of temperature (T) conditions; here T = 298 K.

Electrochemical polarization curves for Ti and colored passive layers on Ti were recorded in 1 wt % aqueous NaCl solution in a standard, two-compartment electrochemical cell. This particular solution concentration of NaCl was chosen in order to: (i) mimic a typical saline environment; (ii) simulate a corrosive environment in which corrosion studies are typically performed; and (iii) simulate a physiological body-type fluid that would normally possess NaCl as the main component.[21,22] During electrochemical characterization, a stream of Ar(g) (99.99 wt %) was passed through the electrolyte to expel any gases generated, as well as to maintain a neutral-gas environment. The reference electrode employed was a Pt/Pt black reversible hydrogen electrode (RHE).

Surface Morphology Characterization. Colored Ti passive layers were studied for uniformity of coloration and morphology by visible light microscopy (VLM) using a Seiwa Optical SDMTR microscope. Surface roughness measurements were performed using a Dektak 8 Stylus Profiler (Veeco Instruments Inc., vertical resolution of 40 nm, horizontal resolution of 3.43 data points/μm). The surface profiler employed a stylus (tip diameter = 12.5 μm); thus, it should be mentioned that, due to the tendency of materials to have varying surface characteristics, there may be an error associated with surface characteristics that is smaller than the stylus tip diameter.

The arithmetic surface roughness (R_a) was calculated according to eq 1

$$R_a = \frac{1}{L}\int_{x=0}^{x=L} |y|\, dx \tag{1}$$

where L represents the scan length in the x direction and y represents the vertical deviation of the surface from the mean height.

UV−vis-NIR Reflectance Spectroscopy. Surface coloration was explored using reflectance spectroscopy recorded with an ultraviolet−visible-near infrared (UV−vis-NIR) light source (DH-2000-BAL), fiber-optically connected to a high-resolution spectrometer (HR-4000, Ocean Optics). The employed light source ranged from 215 to 400 nm (deuterium) and 360−2000 nm (tungsten−halogen), and the spectrometer was able to detect in the 200−1100 nm wavelength (λ) range. The reason for using a combined light source (deuterium, tungsten−halogen) was to eliminate saturation and increase the signal-to-noise ratio. The background reference employed was a specialized mirror (STAN-SSH High-reflectivity Specular Reflectance Standard). During data collection using Spectra Suite (Ocean Optics Inc.) software, integration time was 200 ms, average acquisitions were 50, and boxcar average was 10 data points.

ICP-MS Measurements. Inductively coupled plasma mass spectrometry (ICP-MS) experiments were employed using a Varian 820-MS instrument, with a Dionex 600/BioLC liquid chromatography system that was equipped with a GS50 gradient pump, a Rheodyne 9750E injector and a 50 μL sample loop, used for flow-injection. Specimens were placed in a matrix of the previously discussed 1 wt % aqueous NaCl solution (25.0 mL) and sealed. Samples were generated through taking aliquots over time of equal amounts for analysis. The samples were introduced after a stabilization process described herein. The pump was stabilized by introducing a carrier solution of UHP water for 60 min. The torch was aligned using a tuning solution prepared with 5 μg L^{-1} of Be, Mg, Co, In, Ce, Pb, and Ba in 1 wt % HNO_3 in UHP water. The solution was prepared by dilution from a 10 μg L^{-1} Varian tuning solution (Spectropure, St Louis, Missouri, USA). Cleaning and full optimization procedures were performed (nebulizer, torch, sampler, and skimmer cones), including plasma alignment, mass calibration, mass resolution and trim, detector setup, and ion optic settings. Samples were then run in time-resolved mode (peak hopping) with an uptake rate of 1 mL min^{-1}. Linear regression through origin external calibration was performed using a blank, as well as known concentrations of 1, 10, 50, and 100 ppb. Aqueous NaCl (described above) was used as a blank, and ICP-MS standards (SCP Science, Champlain, New York, USA) were employed in the same NaCl solution makeup. The error value on the slopes of calibration curves was 6830 ± 110 (1.7%). The detection limit was 0.1 μg L^{-1} for the Ti solutions.

Electrochemical Instrumentation and Experiments. The instrumentation employed in order to achieve colored passive layers on Ti was a variable AC power supply (Vector-Vid, Instrument Division, WP32) at a frequency of 60 Hz. The applied V_{AC} was monitored by means of a multimeter (Fluke 45). Conversely, the instrumentation employed in order to study electrochemical properties of the materials was an Autolab model PGSTAT302N potentiostat with NOVA 1.6 electrochemical and corrosion software. Electrochemical polarization curves of wire-shaped Ti electrodes were performed in the −1.0 to 3.0 V versus RHE potential range with a 1 wt % aqueous NaCl electrolyte and a Pt mesh counter electrode of 10 times larger surface area than Ti working electrodes. Current density (j) values are reported with respect to the geometric surface area of Ti electrodes employed.

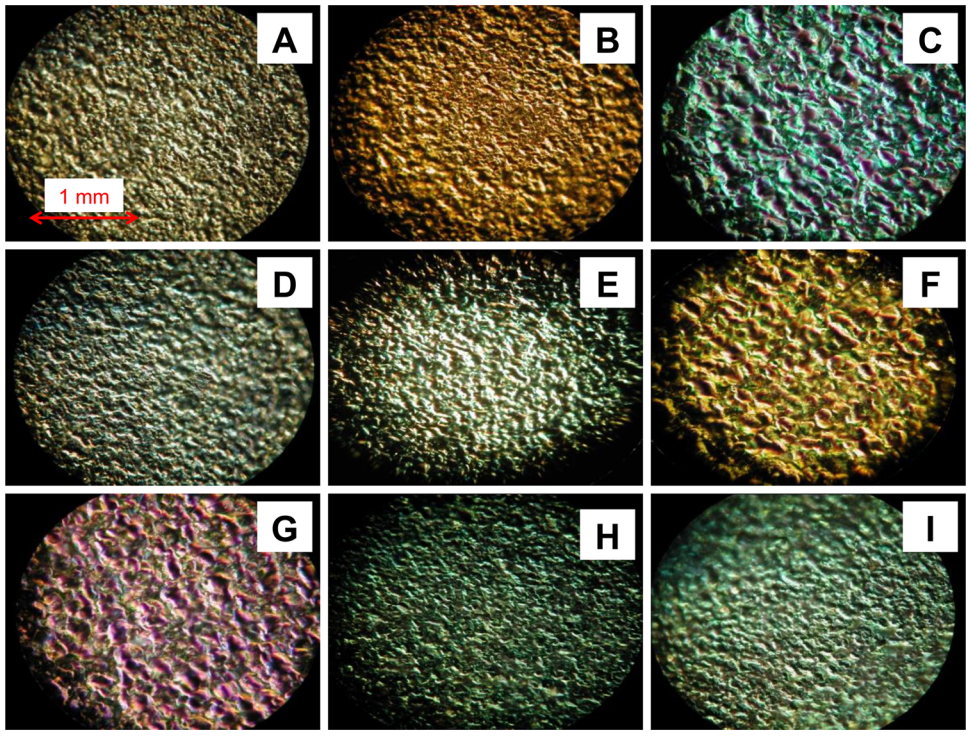

Figure 1. Visible light microscopy images of the colored passive layers on chemically etched Ti formed in 7.5 wt % aqueous NH_4BF_4 solution through the application of AC voltage for 10 s at T = 298 K. Image A presents nonpassivated Ti (V_{AC} = 0 V); images B–I refer to the colored passive layers formed at V_{AC} = 10 (B), 20 (C), ..., 80 V (I), respectively. The magnification is equivalent in each image, and the scale bar is equal to 1 mm.

RESULTS AND DISCUSSION

Coloration and Appearance of Passive Layers on Ti.

Polycrystalline Ti samples were colored by a process described above, involving optimized application of controlled V_{AC}. Specimens were fabricated from as-received Ti wire and sheet material manufactured using pulling and rolling techniques, respectively. Thus, any crystalline characteristics were not identifiable through visual inspection of the mechanically disordered top layer. Post cleaning and etching-procedure samples displayed a well-defined polycrystalline appearance, showing crystallites and grain boundaries. Because of the behavior of each grain as a single crystal (most likely possessing a disordered surface), it was important to assess whether: (i) all crystallites possess equivalent coloration; (ii) there were changes in surface roughness upon passive layer formation, and if so, how it depended on V_{AC}; and (iii) colored passive films revealed cracks or other surface defects that could be assigned to the electrochemical coloring procedure.

Specimens of Ti included mechanically polished and chemically etched Ti, which were necessitated by the desire to examine the influence of surface pretreatment on the colored passive layer development and appearance. Results that display the surface topography variation between pretreatment methods will be discussed further in a later section. However, we were able to determine the average roughness values (R_a) through surface profilometry experiments, which were 0.38 ± 0.04 μm for mechanically polished Ti and 1.29 ± 0.12 μm for chemically etched Ti. Through visual light microscopy (VLM) analysis as well as visual inspection, we observe that there is a noticeable difference between the two types of pretreated samples; thus, we can conclude that sample pretreatment is significant in the passive layer formation process. Samples that underwent mechanical polishing reveal surface scratches, which remain pronounced even after coloration; however, they are very smooth and mirror-like in their appearance as examined by low-magnification VLM. Chemically etched samples produce a matte appearance, as they have a much rougher surface. The process of chemical etching exposes the underlying grain structure developed by Ti during solidification, whereas mechanical polishing elicits a disorder in the outside layers of the Ti material, thus making crystallites challenging to perceive and also introducing potentially previously absent mechanical strain.

Figure 1 presents VLM images, which were obtained using a Seiwa Optical SDMTR microscope, of chemically etched Ti (image A; it serves as a reference) and chemically etched and colored Ti samples (images B–I). The VLM images display that a prominent color emerges despite there often being a varied array of differently colored grains on the surface. Untreated Ti (image A) is gray; however, it also possesses a faint blue coloration. The passive layer formed at V_{AC} = 10 V (image B) has an overall orange coloration with contributions from yellow and red grains. The passive layers formed at V_{AC} = 20 V (image C) and V_{AC} = 30 V (image D) have an overall blue and light blue coloration, respectively. The passive layers also display apparent violet, green, and yellow grains. The passive layer formed at V_{AC} = 40 V (image E) has an overall green coloration, with blue, yellow, and orange contributions. The passive layer formed at V_{AC} = 50 V (image F) has an overall gold-orange coloration with apparent green colored grains. The passive layer produced at V_{AC} = 60 V (image G) is magenta in color due to the violet, green, blue, and red grains. The passive layers formed at V_{AC} = 70 V (image H) and V_{AC} = 80 V (image I) are both teal in coloration due to blue, green, yellow, and orange grains being predominant.

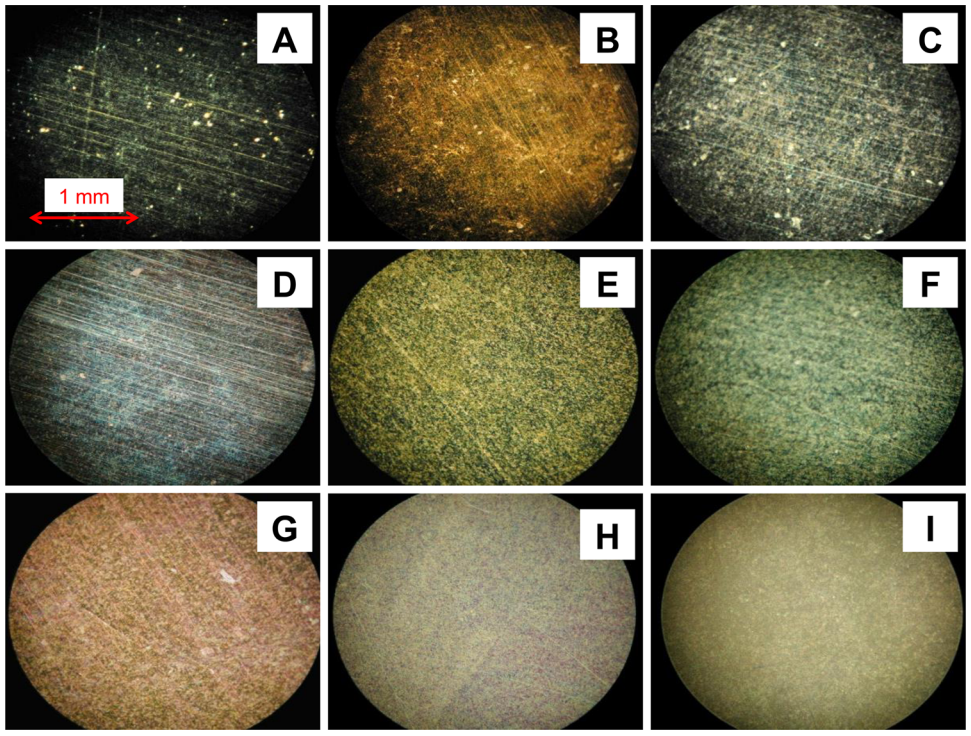

Figure 2. Visible light microscopy images of the colored passive layers on mechanically polished Ti formed in 7.5 wt % aqueous NH_4BF_4 solution through the application of AC voltage for 10 s at T = 298 K. Image A presents nonpassivated Ti (V_{AC} = 0 V); images B–I refer to the colored passive layers formed at V_{AC} = 10 (B), 20 (C), ..., 80 V (I), respectively. The magnification is equivalent in each image, and the scale bar is equal to 1 mm.

Figure 2 presents VLM images of mechanically polished Ti (image A; it serves as a reference) and mechanically polished and colored Ti samples (images B–I). Through comparing these images, it is clear that the surface of passivated Ti is much smoother with mechanical polishing pretreatment than chemical etching pretreatment. The colorations are similar to that of the chemically etched samples; however, there are some samples that show distinct differences. The mechanically polished sample prepared at V_{AC} = 50 V (image F) has a teal appearance under VLM, whereas the corresponding chemically etched sample (Figure 1, image F) showed a golden orange coloration. There are also differences between the mechanically etched and chemically polished samples prepared at V_{AC} = 70 and 80 V. The mechanically polished sample prepared at V_{AC} = 70 V (image H) has an overall violet coloration with blue and green colored grains, whereas the chemically etched sample prepared at V_{AC} = 70 V (Figure 1, image H) displays an overall teal coloration. The mechanically polished sample prepared at V_{AC} = 80 V (image I) has a light-brown coloration overall, whereas the chemically etched sample prepared at V_{AC} = 80 V (Figure 1, image I) has an overall teal coloration. As the etched and mechanically polished samples were colored at the same respective V_{AC}, any variation in coloration can be attributed to the difference in grain orientation and surface disorder due to invasive pretreatment methods, and consequently to different rates of passive layer growth on the two types of samples.

As we previously reported for Zr, samples prepared with V_{AC} > 80 V are not discussed because the application of higher potential results in electrical breakdown of the passive layers, which is accompanied by visible sparking and audible cracking.[21,23,24] The results of VLM measurements may be summarized as follows: (i) In the case of mechanically polished samples, the surface coloration is predominantly uniform. (ii) In the case of chemically etched samples, the varying surface coloration is due to the surface morphology that resembles rolling hills and valleys; because these are interference colors, a varying incidence angle gives rise to different colorations. (iii) Certain grains possess different morphology and display slightly varied coloration from what is expected for a particular V_{AC} value; thus, in this case, the passive layer thickness is not equivalent on each grain. (iv) The colored passive layers are free of micrometer-sized cracks that could be attributed to the formation of the colored passive layer (in the case of the mechanically polished samples, scratches formed on the Ti samples prior to the passive layer formation remain, although they become less-well pronounced as the colored passive layer thickness increases).

Surface Morphology of Colored Passive Layers on Ti. Stylus surface profilometry was employed in order to test the surface roughness and morphology of the colored passive layers on Ti. Average surface roughness (R_a) of the colored passive layers was determined by recording four topography maps (2.5 mm by 2.5 mm) per sample. The resulting R_a values are summarized in Table 1 for two sets of samples: (i) etched and colored titanium; and (ii) polished and colored titanium. As expected, the R_a values demonstrate that the polished samples are less rough than the etched ones; thus, the overall roughness values were representative of the VLM results. Since rougher surfaces have been proven to enable osseointegration of implants, a recommended pretreatment for implant materials would be chemical etching, followed by passivation at a specific V_{AC}, the value of which depends on the optimal R_a value.

UV–vis-NIR Reflectance Spectroscopy. Reflectance spectroscopy measurements were carried out in order to identify wavelength regions of strong intensity and then to compare them with the coloration observed by VLM (Figures 1

Table 1. Surface Profilometry Measurement Results for Average Surface Roughness (R_a) of Untreated and Electrochemically Colored Ti in Relation to the Applied AC Voltage and Surface Pretreatment[a]

V_{AC} (V)	R_a (μm) for etched Ti	R_a (μm) for polished Ti
0	1.29 ± 0.12	0.38 ± 0.04
10	1.20 ± 0.11	0.14 ± 0.04
20	0.85 ± 0.08	0.24 ± 0.04
30	0.95 ± 0.09	0.27 ± 0.04
40	0.82 ± 0.07	0.17 ± 0.04
50	0.90 ± 0.08	0.12 ± 0.04
60	1.04 ± 0.09	0.39 ± 0.04
70	0.81 ± 0.07	0.20 ± 0.04
80	0.81 ± 0.07	0.21 ± 0.04

[a]The sample listed under V_{AC} = 0 V refers to nonpassivated Ti.

and 2). The samples studied are as follows: (i) etched and colored Ti; and (ii) polished and colored Ti. These measurements were conducted in the λ = 200−1100 nm range. Results are displayed as reflectance (R) versus λ, with reflectance defined as $R = I_{refl}/I_{incid}$, where I_{refl} and I_{incid} are the reflected and incident spectral intensities, respectively. Values of R are in the range from 0 to 1, with R = 1 referring to 100% light reflection. We also examined the UV and NIR ranges for interesting spectral features, despite the visible spectrum in the λ = 400−780 nm range being of greatest importance in the analysis of coloration. Reflectance spectra for nonpassivated Ti samples, as well as colored passive layers formed on both etched (left-hand column) and polished (right-hand column) Ti samples, are displayed in Figure 3. Reflectance spectra obtained for etched and polished Ti samples display varying intensities, which is not surprising as Ti, upon solidification, develops large grains and its chemical etching yields a rough surface. Spectra for V_{AC} = 0 V (nonpassivated Ti) serve as references, displaying a trend of R increasing with λ up to 780 nm, which is much more prevalent in the mechanically polished sample. This trend is common for high refractive index materials like metals and is due to the value of refractive index being dependent on wavelength.[21] The reference spectra also show features in the 475−500 nm region, which indicate the presence of contributions from the blue region of visible light. These results are corroborated by VLM results (images A in Figures 1 and 2), which show that untreated Ti has a bluish appearance. Samples prepared at V_{AC} = 10 V have spectra with an overall similar shape, both showing a feature in the 420−500 nm range, which indicates the reflectance of violet and blue light. There are also contributions from yellow, orange, and red producing an overall reddish brown appearance (images B in Figures 1 and 2). The passive layers prepared at V_{AC} = 20 V have reflectance spectra that display a similar shape, both showing a feature in the 440−550 nm range, giving the sample a dark blue appearance (images C in Figures 1 and 2). In the case of V_{AC} = 30 V, the reflectance spectra have a similar overall shape, with very different intensities. The chemically etched sample has a spectrum that shows a feature in the 450−600 nm range, and the spectrum of the mechanically polished sample displays a broad region of high intensity in the 400−780 nm range, producing an overall light blue appearance for both samples (images D in Figures 1 and 2). The reflectance spectra for V_{AC} = 40 V have different intensities, with features in the 475−600 nm range for the etched sample and in the 475−780 nm range for the polished sample. Both samples have an overall

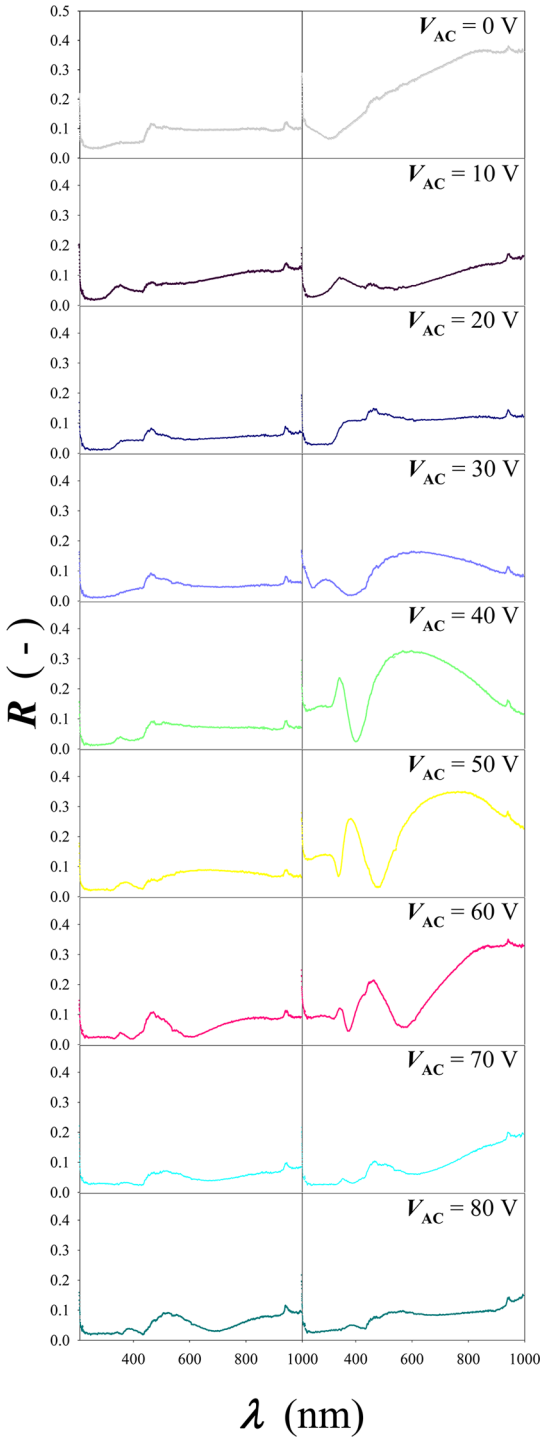

Figure 3. Reflectance spectra (R vs λ) in the λ = 200−1100 nm range for the colored passive layers formed on chemically etched (left-hand column) and mechanically polished (right-hand column) Ti samples. Line colors were chosen in order to present the overall visible coloration.

light green appearance (images E in Figures 1 and 2). Reflectance spectra for V_{AC} = 50 V show differing intensities, with features in the 580−650 nm range for the etched sample and in the 400−445 and 525−780 nm ranges for the polished sample. Both samples have an overall golden orange appearance (images F in Figures 1 and 2). In the case of V_{AC} = 60 V, the reflectance spectra have similar overall shapes, as well as different intensities. The spectra have broad regions of high

dx.doi.org/10.1021/am506572m | ACS Appl. Mater. Interfaces 2014, 6, 21576−21584

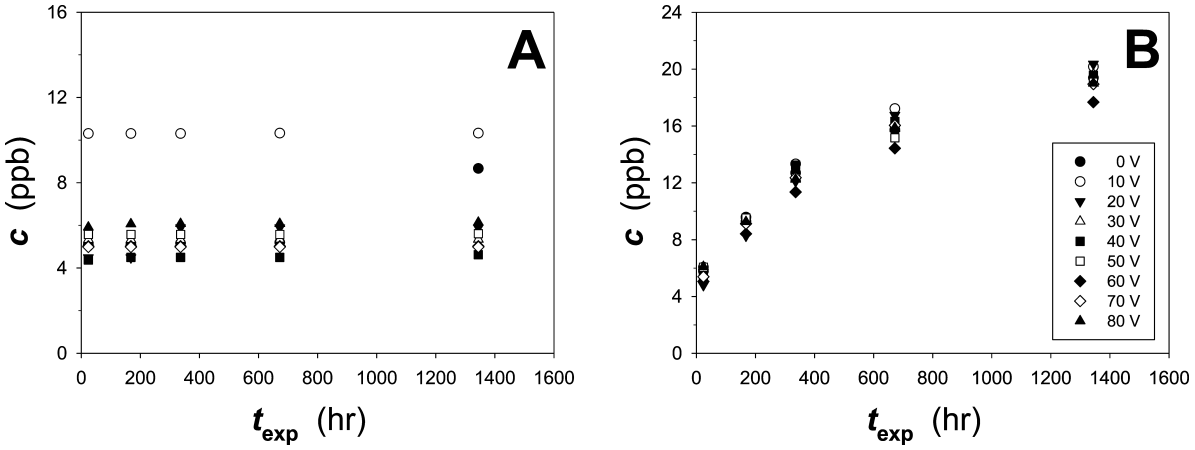

Figure 4. Amount of dissolved Ti through corrosion upon varied exposure to 1 wt % aqueous NaCl solution expressed as concentration (c) in ppb. It is presented as a function of the exposure time (t_{exp}) and V_{AC} for the chemically etched (A) and mechanically polished (B) Ti samples.

intensity in the 400−600 nm range as well as increased R values as λ approaches 780 nm, indicating the presence of violet, blue, green, and red light to generate an overall magenta coloration (images G in Figures 1 and 2). The reflectance spectra for V_{AC} = 70 and 80 V are all very similar in shape, with features in the 450−550 nm regions as well as an increase in R as λ approaches 780 nm. These samples display an overall teal coloration (images H and I in Figures 1 and 2). We observe that the etched and polished Ti samples prepared at the same V_{AC} have the same overall coloration, which is derived from the constructively reflected component colors.

We observe that the application of a given V_{AC} generates similar colorations in the case of etched and polished Ti samples, despite their different textures. This similarity of coloration despite the varying pretreatment methods is due to similar values of thickness of the passive layers. Colored passive layers on etched and polished samples possess distinct textures, which can be attributed to structural differences arising from pretreatment methods. The application of higher V_{AC} results in a red-shift of spectral features toward longer wavelengths. We observe that with a spectral feature shift toward longer wavelength, arises a new feature within the UV range, which indicates that increasing V_{AC} (increasing passive layer thickness) causes different wavelengths to contribute to the constructive and destructive interference.[21]

ICP-MS Analysis. In order to carefully investigate corrosion properties of passivated Ti samples, inductively coupled plasma mass spectrometry studies were performed on chemically etched and mechanically polished Ti samples that were electrochemically passivated ($10 \leq V_{AC} \leq 80$ V). Nonpassivated Ti samples (V_{AC} = 0 V) served as references. Sample preparation was similar to that of our work with passivated Zr,[21] where samples were placed in sealed test tubes containing 25 mL of 1 wt % aqueous NaCl solution for a varied array of exposure times (t_{exp}), up to 8 weeks. Aliquots of the aqueous NaCl solution were collected at the following intervals: 24 h (1 day), 168 h (7 days), 336 h (14 days), 672 h (28 days), and 1344 h (56 days), respectively. We report graphs showing the quantity of dissolved Ti expressed as concentration (c) in ppb as a function of t_{exp} for chemically etched and mechanically polished samples in Figure 4A,B, respectively. The experimental uncertainty associated with the determination of c is ca. 5%. Figure 4 does not contain error bars because the experimental points are close to each other and their addition would obscure the graphs. In general, the amounts of Ti cations are very low and do not exceed 20 ppb, and the longer the t_{exp}, the greater the amount of dissolved Ti. Interestingly, etched and polished samples display slightly different results in this regard. The etched samples (Figure 4A) display that the amount of Ti in the 1 wt % NaCl solution never exceeds 11 ppb. We also observe that nonpassivated Ti samples (filled circles) and the passivated at V_{AC} = 10 V samples have a higher concentration in solution (∼10 ppb) than the Ti samples passivated at $20 \leq V_{AC} \leq 80$ V (ca. 4−6 ppb). In the case of the polished samples (Figure 4B), the amount of dissolved Ti in the 1 wt % aqueous NaCl solution increases gradually over time up to a limiting value of ca. 20 ppb. We also observe that there is practically no difference between the nonpassivated and passivated polished Ti samples. This behavior is assigned to the disordered nature of the Ti surface after mechanical polishing; the corrosion behavior of colored passive layers on polished Ti is similar to that of nonpassivated polished Ti and does not really depend on the colored layer development. In conclusion, these results indicate that the pretreatment method prior to passivation has an impact on the metallic dissolution of Ti in an aqueous saline solution (1 wt % NaCl).

Polarization Curves. In order to further understand the corrosion behavior of Ti in 1 wt % aqueous NaCl solution, and thus to build a better knowledge base of passivated Ti corrosion properties, we recorded potentiodynamic polarization curves for colored passive layers formed on chemically etched Ti. A nonpassivated Ti sample (V_{AC} = 0 V) was employed for comparative analysis. Because of our findings that colored passive layers on mechanically polished samples behave practically the same way as nonpassivated Ti (found through ICP-MS measurements), we focused on etched Ti samples for this study. Figure 5 displays potentiodynamic polarization curves that were recorded in the −1.0 to +3.0 V potential range at a scan rate of s = 1 mV s^{-1} and at a temperature of T = 298 K. The graphs display polarization curves for chemically etched and nonpassivated Ti (gray line), and for a colored passive layer formed at a given V_{AC} (colored line). The images A through H refer to the colored passive layers formed at V_{AC} = 10 (A), 20 (B), ..., 80 V (H), respectively. Analysis of the transients for the passive films reveals the following characteristics: (i) the overall shape of the polarization curves for passive films on Ti is similar; (ii) the polarization curves do not display characteristic features of the active-passive transition;[15,21,25] (iii) the value of j

dx.doi.org/10.1021/am506572m | ACS Appl. Mater. Interfaces 2014, 6, 21576−21584

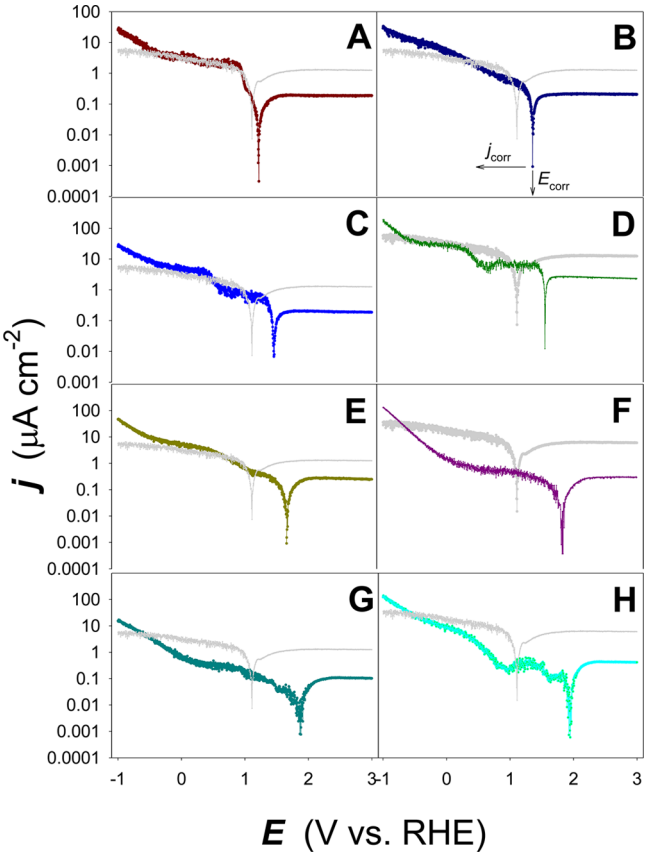

Figure 5. Potentiodynamic polarization curves recorded in 1 wt % aqueous NaCl solution (potential range = −1.0 to +3.0 V, scan rate of s = 1 mV s^{-1}, temperature of T = 298 K). Graphs A−H present two different polarization curves; chemically etched and nonpassivated Ti (gray line) and colored passive layers formed at a given V_{AC} (colored lines). Images A through H refer to the colored passive layers formed at V_{AC} = 10 (A), 20 (B), ..., 80 V (H), respectively

for a colored passive layer, at any given E, is consistently less than that for nonpassivated Ti; (iv) the value of j, at any given E, decreases with increasing V_{AC}; and (v) the corrosion potential (E_{corr}) increases and the corrosion current density (j_{corr}) decreases with the development of a colored passive layer as compared to etched and nonpassivated Ti. We can thus conclude that etched Ti samples coated with colored passive layers are more stable than nonpassivated etched Ti when placed in a 1 wt % aqueous NaCl solution. This finding was similar to that of our previous work with Zr.[21]

In order to further investigate the corrosion properties of the colored passive layers on Ti, we also determined the values of E_{corr} and j_{corr}. Figure 6A demonstrates the variation of E_{corr} with V_{AC} and shows that, with an increase in the thickness of passive layers on Ti (thus with an increase in V_{AC}), E_{corr} also increases from −0.08 V for nonpassivated Ti to +0.29 V for the colored passive layer formed at V_{AC} = 80 V; the relationship between E_{corr} and V_{AC} is linear with a positive slope. The relationship between j_{corr} and V_{AC} is presented in Figure 6B; it displays that the values of j_{corr} are very small. The value of j_{corr} for nonpassivated Ti is 39 nA cm^{-2}, and the values of j_{corr} for colored passive layers never exceed 10 nA cm^{-2}, with the lowest value of 1.3 nA cm^{-2} observed for the colored passive layer formed at V_{AC} = 80 V. The thinnest colored passive layer (V_{AC} = 10 V) displays j_{corr} = 2.1 nA cm^{-2}, which is a significant decrease (18 times) as compared to that of nonpassivated Ti. There is no apparent trend in the j_{corr} versus V_{AC} behavior.

Comparison of the Behavior of Ti and Zr. As we have presented in this study and in our previous study on Zr,[21] the application of AC voltage (AC polarization) to Ti and Zr results in the formation of passive layers that display bright, uniform, and well-defined coloration. The coloration of Ti requires an aqueous solution of NH_4BF_4, while the coloration of Zr an aqueous solution of Na_2SO_4.[14,15] Interestingly, the employment of aqueous solution of NH_4BF_4 to coloring Zr or aqueous solution of Na_2SO_4 to coloring Ti does not produce the same results. VLM analyses displayed that the passive layers are free of any fractures (cracks), flaking, or pits that would originate from the preparation process and would leave the metal vulnerable to corrosion damage. These measurements clearly display the differences between surface pretreatment methods: mechanical polishing and chemical etching. Polished samples of both Zr and Ti display a similar appearance under VLM; however, the etched samples display a distinct difference in surface structure and roughness. Etched Zr samples revealed a relatively smooth overall surface structure,[21] whereas the etched Ti samples revealed a rougher overall surface structure due to the inherent differences in the crystallite sizes. VLM images were also able to reveal the presence of pores due to the onset of electrical breakdown of the passive layers on Zr and Ti prepared at V_{AC} = 60 to 80 V; the electrical breakdown became

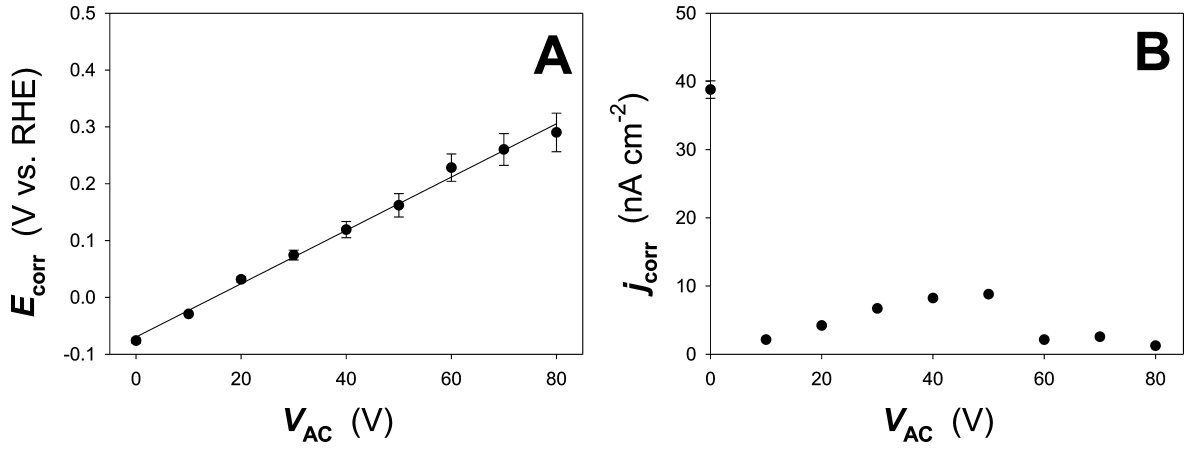

Figure 6. Relationships between E_{corr} and V_{AC} (A) and j_{corr} and V_{AC} (B) for the colored passive layers formed on etched Ti.

dx.doi.org/10.1021/am506572m | ACS Appl. Mater. Interfaces 2014, 6, 21576−21584

increasingly prevalent across the surfaces of Zr and Ti with higher V_{AC} values.[21]

UV−vis-NIR reflectance experiments displayed similar trends between the two metals: (i) a red-shift with increasing V_{AC}; (ii) regions of high intensity and their corresponding wavelengths, which were consistent with the coloration observed using VLM; and (iii) R_a values dependent upon the surface structure, making smoother surfaces (polished samples of Ti and Zr, and etched samples of Zr) more intensely reflective.[21] Zirconium solidification produces small crystallites (each being a single crystal), whereas titanium solidification generates large crystallites. As a result, Ti and Zr display different surface morphologies after etching and, consequently, different trends with their varying colorations and pretreatments. Profilometry experiments further confirmed: (i) the presence of pores developed at higher V_{AC} for both Ti and Zr samples (due to the onset of electrical breakdown); (ii) varying roughness developed by surface pretreatment methods; and (iii) overall roughness values were found to increase with V_{AC}.[16,21]

Corrosion resistance of Zr and Ti was explored by employing ICP-MS and conducting electrochemical experiments. ICP-MS was used to measure metallic dissolution in 1 wt % aqueous NaCl solution. In the case of Ti, the amount of dissolved Ti is very small and hardly depends on the applied V_{AC} or the pretreatment (etching or mechanical polishing). However, the behavior of Zr samples was very different because their corrosion properties strongly depended on their pretreatment, which involves mechanical polishing and chemical etching. The most important observation is that the amount of dissolved metal originating from etched and colored samples was almost 3 orders of magnitude higher than the amount originating from polished and colored samples.[21]

Overall, AC passivation of Ti and Zr in carefully selected aqueous solutions of inorganic salts generates brightly colored and chemically stable layers that offer both protection against corrosion and decorative properties. Their visual appearance (shiny versus matte) can be fine-tuned depending on the end usage. The research outcome outlined in this and past contributions demonstrates that the methodology of preparing colored passive layers on Ti and Zr is ready for a scale-up and eventual industrial implementation.[14−17,21]

CONCLUSIONS

In conclusion, titanium can be successfully colored through the application of AC voltage in an aqueous solution of NH_4BF_4. The colored passive layers on Ti reveal a clear range of well-defined colors that are bright and uniform throughout, arising from iridescence. The passive layer coloration and visual appearance have the potential for facile fine-tuning through changes in the applied AC voltage or employing suitable pretreatment, such as chemical etching, mechanical polishing, or even microsandblasting. Surface morphology analyses were performed using visible light microscopy, revealing the passive layers to be free of surface cracks, flakes, or pits. The surface topography examined using stylus surface profilometry reveals that microroughness on the surface of colored passive layers on Ti is lower than that of nonpassivated Ti. Reflectance spectroscopy allowed for the contributing spectral regions in the visible range to be identified and compared with the overall coloration as determined by visual inspection and visible light microscopy. Corrosion behavior was investigated by inductively coupled plasma mass spectrometry measurements, which were employed in order to quantify the portion of dissolved Ti in the electrolyte (here, 1 wt % aqueous NaCl), as well as electrochemical techniques that determine the corrosion potential and corrosion current density. Samples that were treated with chemical etchant revealed outstanding stability in aqueous saline medium (1 wt % NaCl), with the formation of progressively thicker colored passive layers improving their resistance to corrosion. The stability of polished and colored Ti samples revealed similar stability to the etched samples, but the corrosion behavior was more related to the mechanically disordered outer layer than due to passivation. In the case of etched Ti samples, the outcome of electrochemical measurements supported the results of inductively coupled plasma mass spectrometry measurements by demonstrating that the colored passive layers on Ti increase the corrosion potential and decrease the corrosion current density; thus, with thicker passive layers, there is additional stability as compared to untreated Ti. An innovative aspect of the work reported here is the application of inductively coupled plasma mass spectrometry to corrosion studies. The colored passive layers offer outstanding visual properties to a metal that possesses remarkable physical properties and open a new range of applications.[26,27]

AUTHOR INFORMATION

Corresponding Authors

*E-mail: gregory.jerkiewicz@chem.queensu.ca (G.J.).
*E-mail: diane.beauchemin@chem.queensu.ca (D.B.).

Notes

The authors declare no competing financial interest.

ACKNOWLEDGMENTS

We gratefully acknowledge financial support toward this project from the NSERC of Canada (Discovery Grant and Research Tools and Instruments Grants).

REFERENCES

(1) Boyer, R.; Collings, E. W.; Welsch, G. *Materials Properties Handbook: Titanium Alloys*, 1st ed.; ASM International: Materials Park, OH, 1994.
(2) Barksdale, J. In *The Encyclopedia of the Chemical Elements*; Hampel, C. A., Ed.; Reinhold Book Corporation: New York, 1968.
(3) Codell, M. *Analytical Chemistry of Titanium Metals and Compounds*; Interscience Publishers Inc.: New York, 1959.
(4) Donachie, M. J. *Titanium: A Technical Guide*; ASM International: Materials Park, OH, 2000.
(5) Emsley, J. *Nature's Building Blocks: An A-Z Guide to the Elements*; Oxford University Press: Oxford, U.K., 2001.
(6) Schutz, R. W.; Covington, L. C. Effect of Oxide-Films on the Corrosion-Resistance of Titanium. *Corrosion* **1981**, *37*, 585−591.
(7) Lausmaa, J.; Kasemo, B.; Mattsson, H.; Odelius, H. Multitechnique Surface Characterization of Oxide-Films on Electropolished and Anodically Oxidized Titanium. *Appl. Surf. Sci.* **1990**, *45*, 189−200.
(8) Delplancke, J. L.; Degrez, M.; Fontana, A.; Winand, R. Self-Colour Anodizing of Titanium. *Surf. Technol.* **1982**, *16*, 153−162.
(9) Delplancke, J.-L.; Winand, R. Galvanostatic Anodization of Titanium—I. Structures and Compositions of the Anodic Films. *Electrochim. Acta* **1988**, *33*, 1539−1549.
(10) Delplancke, J. L.; Winand, R. Galvanostatic Anodization of Titanium—II. Reactions Efficiencies and Electrochemical Behaviour Model. *Electrochim. Acta* **1988**, *33*, 1551−1559.
(11) Gaul, E. Coloring Titanium and Related Metals by Electrochemical Oxidation. *J. Chem. Educ.* **1993**, *70*, 176−178.
(12) Petit, J. A.; Chatainier, G.; Dabosi, F. Inhibitors for the Corrosion of Reactive Metals: Titanium and Zirconium and Their Alloys in Acid Media. *Corros. Sci.* **1981**, *21*, 279−299.

(13) Delplancke, J.-L.; Sun, M.; O'Keefe, T. J.; Winand, R. Nucleation of Electrodeposited Copper on Anodized Titanium. *Hydrometallurgy* **1989**, *23*, 47−66.
(14) Hrapovic, S.; Luan, B. L.; D'Amours, M.; Vatankhah, G.; Jerkiewicz, G. Morphology, Chemical Composition, and Electrochemical Characteristics of Colored Titanium Passive Layers. *Langmuir* **2001**, *17*, 3051−3060.
(15) Jerkiewicz, G.; Strzelecki, H.; Wieckowski, A. A New Procedure of Formation of Multicolor Passive Films on Titanium: Compositional Depth Profile Analysis. *Langmuir* **1996**, *12*, 1005−1010.
(16) Zhao, B.; Jerkiewicz, G. A New Procedure of Formation of Multicolor Passive Films on Titanium: Compositional Depth Profile Analysis. *Can. J. Chem.* **2006**, *84*, 1132−1145.
(17) Zhao, B.; Jerkiewicz, G.; Hrapovic, S.; Luan, B. Discovery of Reversible Switching of Coloration of Passive Layers on Titanium. *Chem. Mater.* **2008**, *20*, 1877−1880.
(18) Li, D. H.; Ferguson, S. J.; Beutler, T.; Cochran, D. L.; Sittig, C.; Hirt, H. P.; Buser, D. Biomechanical Comparison of the Sandblasted and Acid-Etched and the Machined and Acid-Etched Titanium Surface for Dental Implants. *J. Biomed. Mater. Res.* **2002**, *60*, 325.
(19) Lausmaa, J.; Kasemo, B.; Mattsson, H. Surface Spectroscopic Characterization of Titanium Implant Materials. *Appl. Surf. Sci.* **1990**, *44*, 133−146.
(20) Diamanti, M. V.; Pedeferri, M. P.; Schuh, C. A. Thickness of Anodic Titanium Oxides as a Function of Crystallographic Orientation of the Substrate. *Metall. Mater. Trans. A* **2008**, *29A*, 2143−2147.
(21) Holmberg, R. J.; Bolduc, S.; Beauchemin, D.; Jerkiewicz, G.; Schulz, H.; Kohlhaas, U.; Strzelecki, H. Characteristics of Colored Passive Layers on Zirconium: Morphology, Optical Properties and Corrosion Resistance. *ACS Appl. Mater. Interface* **2012**, *4*, 6487−6498.
(22) Huang, Y. Z.; Blackwood, D. J. Characterisation of Titanium Oxide Film Grown in 0.9% NaCl at Different Sweep Rates. *Electrochim. Acta* **2005**, *51*, 1099−1107.
(23) Kalra, K. C.; Singh, K. C.; Singh, M. Electrical Breakdown of Anodic Films on Titanium in Aqueous Electrolytes. *J. Electroanal. Chem.* **1994**, *371*, 73−78.
(24) Sul, Y.-T.; Johansson, C. B.; Petronis, S.; Krozer, A.; Jeong, Y.; Wennerberg, A.; Albrektsson, T. Characteristics of the Surface Oxides on Turned and Electrochemically Oxidized Pure Titanium Implants up to Dielectric Breakdown: The Oxide Thickness, Micropore Configurations, Surface Roughness, Crystal Structure and Chemical Composition. *Biomaterials* **2002**, *23*, 491−501.
(25) Laser, D.; Yaniv, M.; Gottesfeld, S. Electrochemical and Optical Properties of This Oxide Layers Formed on Fresh Titanium Surfaces in Acid Solutions. *J. Electrochem. Soc.* **1978**, *125*, 358−365.
(26) Kibayashi, H.; Ogihara, H.; Hayano, Y.; Saji, T. Hard and Glossy-Colored Films Composed of Micropatterned Organic Dots and Electrodeposited Honeycomb-Shaped Nickel Walls. *ACS Appl. Mater. Interface* **2012**, *4*, 590−592.
(27) Erol, M.; Dikici, T.; Toparli, M.; Celik, E. The Effect of Anodization Parameters on the Formation of Nanoporous TiO_2 Layers and Their Photocatalytic Activities. *J. Alloys Compd.* **2014**, *604*, 66−72.